System for ESR measurements at hydrostatic pressures to 60 kilobars[a)]

J. Dean Barnett, Som D. Tyagi,[b)] and H. Mark Nelson

Department of Physics and Astronomy, Brigham Young University, Provo, Utah 84602

(Received 28 September 1977)

A single-crystal sapphire serves both as a solid microwave cavity (X band) and an anvil in a Bridgman-anvil pressure geometry. A metal gasket is used in a manner similar to its use in the diamond-anvil pressure cell, and single-crystal samples are subject to purely hydrostatic pressures. The ruby-fluorescence pressure–measurement technique is utilized. Sample size is limited to a disk approximately 0.6 mm in diameter and 0.1 mm thick. ESR data on Cr^{3+} in ruby to 60 kilobars are given as an illustration of the precision and data quality. Line widths and profiles, as well as line positions, are meaningful. Very little degradation of the data is experienced at the higher pressures. The first and second derivatives of the zero-field splitting (δ) of the states in ruby with pressure are measured as $d\delta/dP = (6.70 \pm 0.08) \times 10^{-4}$ $cm^{-1}kilobar^{-1}$ and $d^2\delta/dP^2 = (-2.44 \pm 0.30) \times 10^{-6}$ $cm^{-1}kilobar^{-2}$ at $P = 0$. The gyromagnetic ratio $g_{\parallel}$ is shown to experience a fractional change less than 2×10^{-4} to 60 kilobars.

INTRODUCTION

The use of the electron spin resonance technique in the studies of the microscopic local fields in solids has been of significant value in the fundamental understanding of a variety of materials and phenomena. The high sensitivity and local nature of the measurement make it particularly valuable in studies involving microscopic mechanisms.

In recent years extensive experimental studies of the properties of solids subjected to high pressures sufficient to change interatomic distances significantly have been carried out to clarify and elucidate the theoretical dependence on the atomic separation. ESR studies as a function of temperature are now rather routine in many laboratories, and such studies have been most useful. From a fundamental quantum standpoint, measurements with varying pressure give uniquely different data than measurements at varying temperature. The variation of volume (or lattice constant in noncubic materials) changes the external constraints on the quantum system and thus changes the actual quantum states of the system, whereas changes in temperature ideally (isochorically) change only the quantum-level occupation. It is, therefore, of fundamental significance to study the volume dependence in conjunction with the temperature variations and to separate the volume effects from the unique temperature effects. In our laboratory we are specifically interested in a study of the microscopic mechanisms of phase transitions and critical phenomena and have developed this ESR system to carry out such studies. It is apparent that a variation of both the temperature and pressure environments is necessary if one desires to study volumetric effects on critical phenomena. Furthermore, for many materials one must operate in the thermodynamic region where the critical phenomena occur.

Techniques to make ESR measurements at moderately high hydrostatic pressures have been described,[1–3] and measurements at very high quasi-hydrostatic pressures were developed in this laboratory several years ago.[4,5] The lack of truly hydrostatic pressures, however, restricted the use of the higher-pressure system to studies of very strong materials and raised questions in data analysis relative to the effect of any nonhydrostatic stresses. Furthermore, pressure measurements were obtained using fixed-point electrical-resistance changes. The lack of a continuous pressure measuring technique and the experimental difficulties attendant to the electrical-resistance measurement in the earlier system seriously limited the versatility and hampered its use in a routine manner.

The system described herein represents a major modification of the earlier system but still utilizes the X-band Varian spectrometer. The sample now experiences truly hydrostatic pressures, and pressure measurements can now be made rapidly on a continuous scale with precision of approximately 0.3 kilobars. The quasi-hydrostatic environment characteristic of the previous system restricted the data analysis to studies of ESR line positions, whereas the hydrostatic environment allows interpretation of line shapes and line intensities in terms of physically meaningful phenomena. This feature enhances the value of the technique appreciably and qualifies it for studies of the more subtle and fundamental properties of solids as the interatomic distances are changed.

The maximum pressure and temperature capabilities of the system have not been thoroughly studied. We have carried out extensive studies at room temperature to approximately 30 kilobars and have reached pressures of 60 kilobars in an initial attempt at higher-pressure generation. The total pressure cell (described later in detail) can be heated or cooled. Studies carried out

 0034-6748/78/4903-0348$00.60

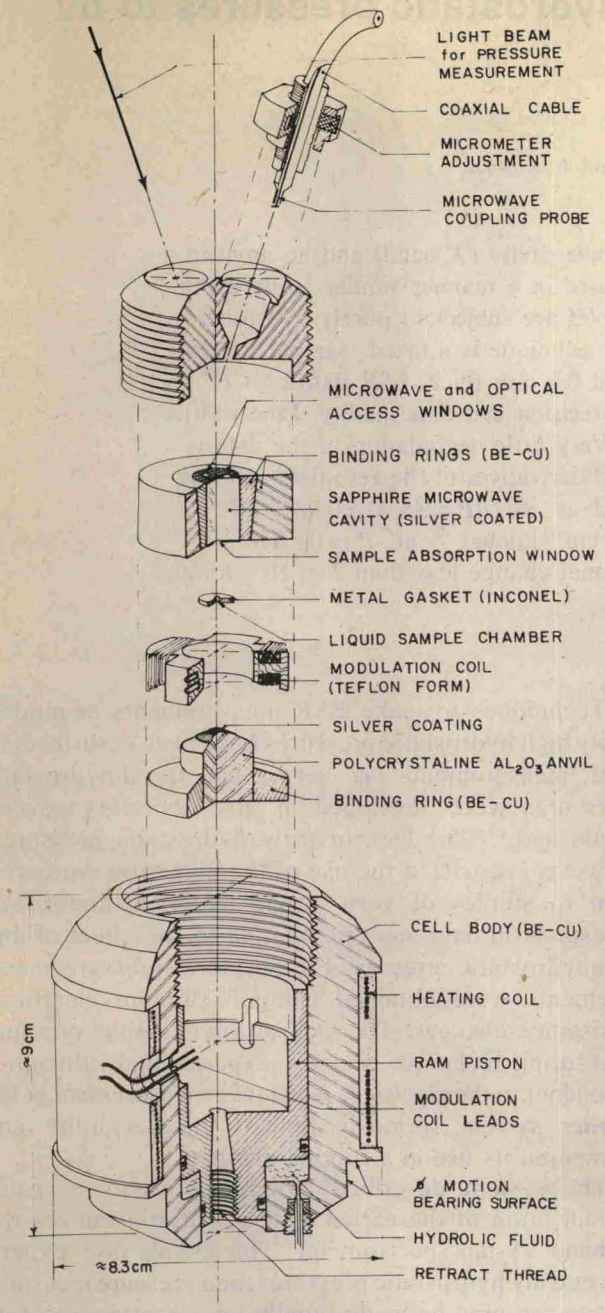

FIG. 1. ESR high-pressure cell illustrating the sapphire resonance cavity, modulation coil, microwave coupling probe, sample chamber and hydraulic-ram assembly.

using the system have largely been at room temperature with limited measurements at temperatures to 200 °C. Serious complications would arise if temperatures above 300 °C or very low temperatures were utilized in the present system. The system has been extensively used to study single-crystal samples under hydrostatic environment but could also be used to study liquids or solutions at high pressures with no modifications at all.

We will first describe the pressure cell which contains a sapphire microwave cavity as an integral part. A discussion of the operation and limitations of the cell will accompany the description. We will then describe the pressure-measuring technique which was recently developed by one of the authors and collaborators[6,7] for use with the diamond-anvil pressure system. Finally, we will present a limited amount of ESR data on ruby to 60 kilobars as an illustration of the potential of the system.

We have already completed a rather extensive ESR study of $CaCO_3$-II, a high-pressure modification of calcite. Calcite transforms to $CaCO_3$-II at approximately 16 kilobar with a first-order displacive transformation (single crystal to single crystal). The results of this study will be published elsewhere.

I. DESIGN OF ESR PRESSURE CELL

The major concept involved in the design of the very high-pressure ESR instrumentation is the use of a high-strength material (sapphire) as both an anvil in a Bridgman-anvil metal-gasketed pressure system and also as a solid dielectric microwave cavity. A cylindrical anvil is coated with a conductive silver layer, and the dimensions (1.25 cm in diameter and 1.78 cm length) are selected to be consistent with the wavelength of the microwave radiation within the dielectric. This cavity is excited either in the TM_{111} or the TM_{110} cylindrical-cavity mode as discussed below. (See Fig. 2.) The silver coating which forms the walls of the cavity is removed from a small area (approximately 1 mm in diameter) at the center of one end of the cavity, and the sample is placed on this area.

If significant pressures are to be obtained, the selection of both the cavity anvil material and the opposing anvil material is crucial. Sapphire has one of the highest compressive strengths of any known crystalline dielectric material. Sintered polycrystalline Al_2O_3 has a higher strength than the single-crystal sapphire since the latter cleaves. We have used single-crystal sapphire for the cavity for reasons discussed later and sintered Al_2O_3 for the opposing anvil.

Having the basic concept for a high-pressure ESR system, one must then consider the less critical features of such a high-pressure system and such an ESR system so that they will be compatible and still yield the highest quality data possible.

A list of items to be considered in a design follows: (a) microwave coupling, (b) magnetic-field modulation, (c) extraneous signals from impurities in the solid cavity, (d) orientational versatility and accuracy, (e) freedom from magnetic materials in the construction, (f) radial support of anvils to increase pressure capabilities, (g) pressure measurement, (h) hydrostaticity of sample environment, (i) sample volume allowed, and (j) temperature capabilities (both low and high).

The system discussed herein and illustrated in an expanded view in Fig. 1 represents our approach to the above considerations in which the following items were dominant objectives: (1) the highest pressures consistent with a truly hydrostatic environment, (2) a continuous pressure-measuring capability, (3) the greatest possible orientational versatility consistent with items (1) and (2),

and (4) some reasonable variation in operating temperatures, particularly at temperatures above ambient temperature. Systems with more moderate pressure capabilities but with low-temperature capabilities could be designed.

The desire for very high pressures dictates a Bridgman-anvil approach. The truly hydrostatic condition requires the use of single-crystal sapphire as an anvil and cavity since sintered Al_2O_3 is pervious to liquids at very high pressures, and thus the liquid cannot be contained. The use of the optically clear single crystal also simplifies the pressure measurements using the ruby-fluorescence technique as discussed later. Furthermore, the purity of the single-crystal sapphire is much greater than the sintered Al_2O_3; thus, we avoid spurious signals from impurities within the cavity. The opposing anvil is made of sintered Al_2O_3 as a cost consideration but also to allow the use of an anvil without radial support. This geometry leaves room for the modulation coils, as illustrated in Fig. 1. The opposing anvil is covered with silver in order to prevent liquid leakage and also to isolate impurities in the opposing anvil from the active microwave cavity.

An eight-ton force-capacity hydraulic ram with a very short (6 mm) travel is incorporated directly within the cell, and a small-diameter (0.5 mm i.d. 1.6 mm o.d.) high-pressure tubing transmits oil pressure to the ram. The total cell rests in an Eulerian cradle to provide essentially arbitrary orientational versatility relative to the magnetic field. Single-crystal orientational studies can thus be made by rotating the entire cell. The stainless-steel pressure tubing is not totally rigid and is coiled into a 1.5-cm-diam coil spring near the input to the cell. This arrangement permits orientational motion of the cell while the sample is under pressure. The Eulerian cradle is constructed such as to totally fit within the 10-cm gap of the 30-cm-diam pole faces of an Electromagnetic Industries electromagnet.

The high pressures are created when a metal gasket with a sample and liquid enclosed is squeezed between the tapered opposing anvil and the sapphire cavity. The technique is similar to that commonly used in the gasketed diamond-anvil pressure cell.[8] The flat face of the tapered anvil is between 2 and 5 mm in diameter, depending upon the maximum pressure desired, and the initial dimensions of the sample chamber range between 0.8 and 1.5 mm in diameter and 0.3 and 0.6 mm in thickness. Smaller anvils must be used to obtain higher pressures since the breakage of sapphire anvils is limited not only by maximum pressures but also by maximum total load. Single-crystal sapphire has been used in a similar manner to over 80 kilobars in a high-pressure Raman apparatus but with slightly smaller samples.[9] Sample thickness must be as small as 0.1 mm to avoid being smashed at the very highest pressures. Samples 0.2 mm thick are usable to 30 kilobars. The yield strength of the gasket material strongly influences the attainable pressures and the chamber size at the maximum pressures. All metal parts of the pressure

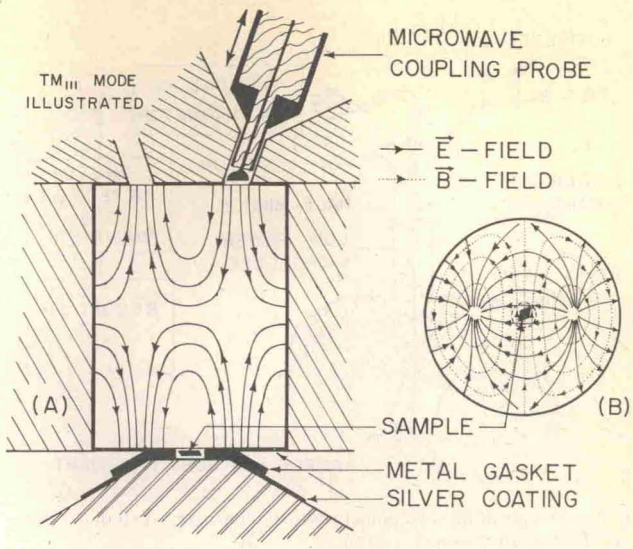

FIG. 2. Details of microwave cavity mode, coupling probe, and sample chamber.

cell are constructed from heat-treated beryllium–copper alloy.

Cracking of the sapphire-anvil cavity limits the pressure capabilities of the cell. The crystallographic c axis of the sapphire is along the axis of the cylinder (±2°), and radial support is provided by the binding rings indicated in Fig. 1. The two binding rings are tapered with a half-cone angle of 0.6°, and an interference of 0.06 to 0.08 mm on the diameter is used to provide maximum support. Care must be taken not to give excessive radial support, or the sapphire may be cracked when assembling the binding rings.

The modulation coils are placed as close to the sample as possible. These coils have an inductance (3.2 mH) and resonant frequency similar to the values for the commercial Varian cavity coils in order to match the impedance of the Varian modulation system. Shielded leads to the 100-kc frequency modulation coil are brought through the ram cylinder walls as indicated in Fig. 1.

Microwave coupling is capacitive in nature and is accomplished by placing a flat tip on the center wire of a high-impedance coaxial input cable at points of high electric field for the specific mode desired on the end of the microwave cavity. The coupling is adjusted by changing the position of this probe relative to the access window provided. The cavity field and coupling are illustrated in Fig. 2. Coupling is very sensitive to the position of the probe, and the flattened probe must be within less than one mm before measurable coupling occurs. The probe has a micrometer adjustment and is adjusted for optimal coupling before each measurement. The coaxial cable is approximately 20 cm long and is connected directly to a wave guide associated with the Varian detection system. In Fig. 2 we illustrate the TM_{111} mode. With this coupling geometry one could, in theory, couple to any TM_{11n} mode. We have observed the TM_{110}, TM_{111}, and TM_{112} modes. Each of these modes

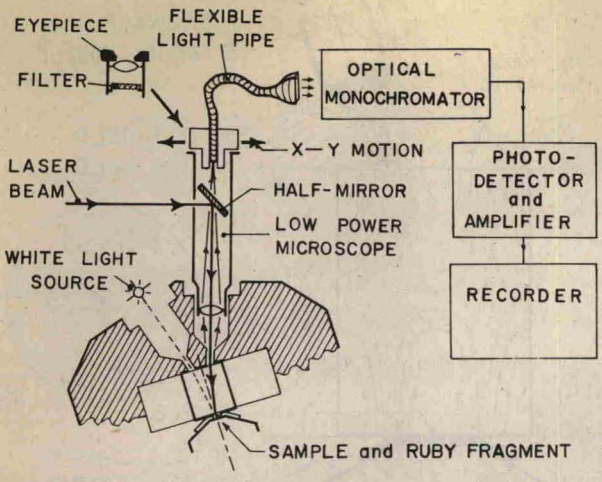

FIG. 3. Details of fluorescence pressure-measuring system as applied to the ESR high-pressure system.

has a maximum **B** field at the center of the cylinder end wall where the sample is placed. The field is slightly perturbed at this point due to the hole in the coating removed to accommodate the sample. When a proper silver coating is applied to the cavity, the TM_{110} mode has a Q of approximately 2500; the TM_{111} has a Q of approximately 2000, and the TM_{112} has a Q of less than 500. Because of the higher Q, the TM_{110} mode is generally used. A second reason for using the TM_{110} is its lack of frequency dependence on the length of the cavity. Experimental measurements of the mode frequency under load indicate a small variation of less than 0.05% up to 60 kilobars. The variation is more dependent on gasket geometry and the changing dimensions and electrical properties in the vicinity of the sample than on the applied load. There is a very sizable variation of the mode frequency with temperature (0.7% for 100 °C temperature change). The temperature shift is apparently related to a variation in dielectric constant of the sapphire.

The coaxial cable and the flexible high-pressure tubing allow orientational movement of the cell, and thus of the enclosed sample in the **B** field, over a range as high as ±60° in any arbitrary direction using the Eulerian cradle. The optimum orientation of the cell for ESR study, however, is when the cavity **B** field at the sample is perpendicular to the magnetic gross **B** field and the modulation **B** field is parallel to the gross **B** field. When the pressure cell is rotated, the cavity field and the modulation field become disoriented from optimum, and the signal intensity deteriorates seriously. Thus, in actual practice, disorientations greater than ±45° are seldom used.

In many applications only minor orientational capabilities are needed, but in studying phase transformations, particularly in noncubic materials, the orientational versatility is important. The new phase may have principal axes oriented in significantly different directions from the original axes.

As seen in Fig. 1, a heating coil was provided as an integral part of the cell. This feature is directly related to the interest at our laboratory in phase-transformation studies. The O-rings in the hydraulic-ram system are high-temperature (300 °C) O-rings, and the modulation-coil form and wire insulation are Teflon. Wire connectors in the modulation coil were made with high-temperature solder. To prevent excessive heat loss to the Eulerian-cradle goniometer in which the cell rests, some nominal thermal insulation was provided between the cell and the cradle. Measurements below room temperature have not been attempted, but for modest decreases in temperature we feel that a cold bath using the enclosed heater to control temperature would be very satisfactory. The hydraulic ram is not spring-loaded, and a thread is provided to allow retraction of the ram by inserting a bolt.

II. APPLICATION OF RUBY-FLUORESCENCE PRESSURE MEASUREMENT

The basic features of the ruby-fluorescence pressure-measuring system involve placing a small ruby fragment (0.05 mm or larger mean dimension) in the pressure cell, illuminating it with high-intensity light, and measuring the wavelength of the R_1 line in the fluorescence spectrum. This wavelength has a nearly linear pressure dependence and has been well calibrated.[7] The technique is well-described elsewhere.[6]

The ESR pressure cell was specifically designed to facilitate the use of the ruby-fluorescence technique of measuring pressure since the utility of the cell would be drastically curtailed if such a continuous pressure-measuring technique were not available.

The essential features of the fluorescence system are shown in Fig. 3. The use of a laser for excitation and a flexible optical light-fiber bundle for transmitting the light from the microscope to the monochromator have now become common. To improve collecting efficiency, the fiber bundle used here incorporates a circle input from the microscope and a slit output to the monochromator as indicated in Fig. 3. This arrangement provides higher light-gathering potential while maintaining spectral resolution in the monochromator. The use of a reflected-light illumination system rather than a transmitted-light configuration is necessary due to the use of a polycrystalline Al_2O_3 as one of the anvils in the pressure system as discussed above. As illustrated in Fig. 3, optical access to the sample is made through the sapphire ESR cavity via the microwave-coupling window. The insertion of the microwave-coupling probe at the angle illustrated is a consequence of the required light path for the laser beam and the location of the cavity-coupling windows specified by the electric-field antinodes for the microwave cavity mode used. Two possible optical or microwave entrance windows are provided for two reasons: First, to facilitate positioning of the laser beam onto the ruby-fluorescing fragment, an auxiliary white light beam is projected into one window while observing with an eyepiece

through the other. An independent access for this white light is necessary because the aperture is so limited that standard microscopic reflection illumination produces excessive background scattered light. This excessive background destroys the optical image. Second, the angular orientational capabilities of the cell are increased if the microwave probe is shifted from one to the other available locations. A short-wavelength cutoff optical filter carefully selected to have a cutoff near the laser wavelength is used in the eyepiece. A filter which passes less than 1% of the laser beam protects the eyes of the experimenter but allows him to see the location where the laser beam is striking and facilitates directing the beam onto the ruby fragment.

The laser is a 15-mW Liconix 401 He–Cd blue (4416 Å) laser. The monochromator is a McPhearson 0.3-m, $f/5.3$ model number (218) system with standard photomultiplier detector. This pressure-measuring system provides reproducible measurements with a precision of approximately 0.3 kilobars by simply reading the ruby line position from a recorder trace. It is important that the laser beam direction and position be adjustable with reasonably high precision to facilitate directing the beam onto the ruby fragment within the pressure cell since the cell cannot be moved easily. A low-precision $x-y$ translator allows the movement at the input end of the light pipe to maximize the signal output of the photodetector.

III. ILLUSTRATIVE ESR MEASUREMENTS ON RUBY

To illustrate the capabilities of the ESR pressure system, we report here some ESR data on ruby. Ruby was chosen as an illustrative example since it yields a relatively simple ESR pattern, and it has been studied extensively at zero pressure.[10–14] Furthermore, previously reported pressure measurements in a hydrostatic environment to 7 kilobars[15,16] give conflicting results with data in a nonhydrostatic environment at pressures to 76 kilobars.[5] The study of ruby is also simplified since the sample itself becomes the pressure sensor using the fluorescence technique. We illustrate two aspects of the data: first, the ability to measure resonance line positions from which crystal field parameters can be extracted; second, the ability to measure line widths and shapes which have meaningful physical significance.

The resonance lines of the Cr^{3+} in ruby represent transitions between Zeeman-split states of spin 1/2 and spin 3/2 which are separated in energy by an amount δ at zero magnetic field. Measurements with **H** along the hexagonal crystal axis yield only three resonance lines corresponding to transitions $+3/2 \rightarrow +1/2$, H_1; $-1/2 \rightarrow +1/2$, H_2; $+1/2 \rightarrow +3/2$, H_3; from this δ can be determined,

$$\delta = h\nu\,(H_1/H_2 + 1) = h\nu\,(H_3/H_2 - 1). \qquad (1)$$

The gyromagnetic ratio of the unpaired electron in this crystalline direction is designated $g_{\parallel}$ and can be determined from

$$g_{\parallel} = \frac{h\nu}{\beta H_2} = \frac{h\nu}{\beta(H_3 - H_1)/2}. \qquad (2)$$

Experimental values of $\delta(P)$ and $g_{\parallel}(P)$ are shown in Figs. 4(a) and 4(b), respectively. Figure 4(c) indicates measured line widths of the three resonances as a function of pressure. The solid line shown in Fig. 4(a) is a least-square fit to the quadratic curve

$$\delta = A + BP - CP^2,$$

with

$$A = 0.38345 \pm 0.00008\ \text{cm}^{-1},$$

$$B = (6.70 \pm 0.08) \times 10^{-4}\ \text{cm}^{-1}\ \text{kilobar}^{-1},$$

and

$$C = (1.22 \pm 0.15) \times 10^{-6}\ \text{cm}^{-1}\ \text{kilobar}^{-1},$$

and the errors are standard deviations taken from the error matrix.

The samples studied were 0.05% molecular concentration of Cr. Each magnetic field was measured with an NMR gaussmeter, and the klystron frequencies were calibrated through a frequency counter traceable to the WWVB frequency standard, both with accuracies of 1×10^{-4}. Thus, the major error in δ and $g_{\parallel}$ is associated with reading errors from recorder traces and associated electronic zero drift. One small but significant systematic error in determining H, which would be of the order of a few parts in 10^4, will be discussed later.

Each point shown in both Figs. 4(a) and 4(b) is the average of two values of δ and $g_{\parallel}$, each calculated using two different lines as indicated in Eqs. (1) and (2), respectively. These values differ on the average by less than two parts in 10^4, and similar differences are observed at the higher pressures as at the lower pressures. We conclude that the errors both systematic and random are typical of the ESR system and are not seriously degraded by the pressure apparatus. The scatter from the least-square fit curve in Fig. 4(a) is approximately twice the error suggested above in measurements of δ. This scatter is principally due to error in pressure measurement. For the data presented here, the uncertainty in pressure is estimated to be 0.5 kilobars and is random in nature. The relatively low Cr concentration in the ruby decreases the fluorescence radiation and lowers the precision of the pressure measurement from the 0.3 value suggested earlier. Using these estimated errors, the error flags in Fig. 4(a) are approximately the size of the points shown.

The precision of the ESR measurement itself is illustrated quite well in the $g_{\parallel}$ data. It is apparent that this parameter is very pressure insensitive, and thus only magnetic-field and klystron-frequency measurements give rise to errors. The random error is seen to be of the order of one part in 10^4. The absolute accuracy of the magnetic-field measurement, however, is based on the NMR calibration of the field without the pressure cell in place. The presence of any magnetic

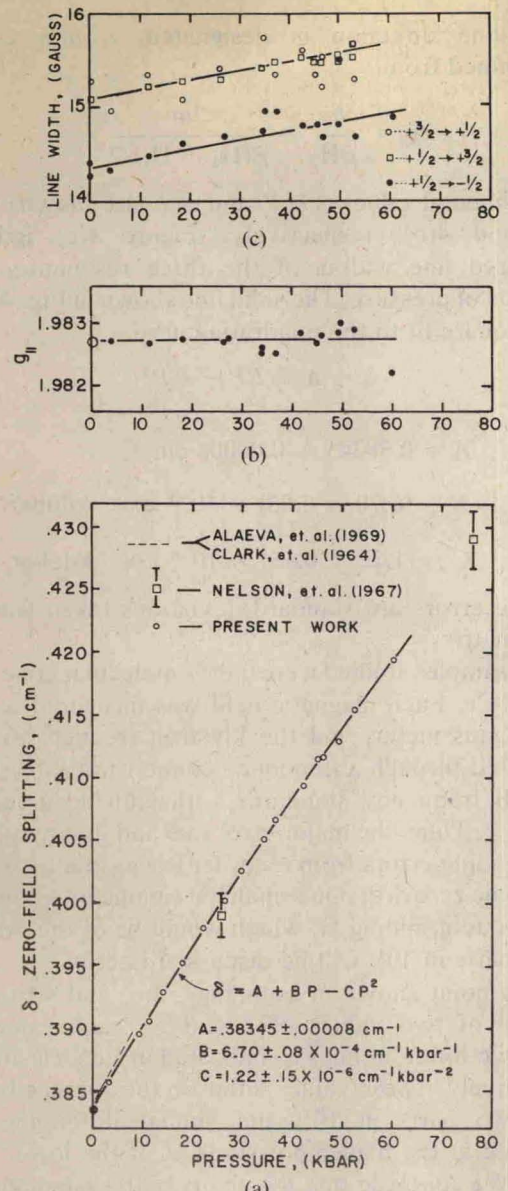

FIG. 4. ESR data on ruby at high pressure illustrating the precision available in measuring both spin-hamiltonian parameters and line widths.

materials in the cell would change the field. The only element in the cell which is not diamagnetic is the metal gasket, which is composed of one of a variety of Inconel alloys of varying strengths depending on the maximum pressure desired. These alloys have magnetic susceptibilities between 1.002 and 1.005 and thus distort the field slightly near the sample. Measurements at zero pressure with and without a gasket surrounding the ruby sample demonstrate no measurable line-broadening effects but a measurable line shift of between 2 and 5×10^{-4}, depending on gasket alloy. Since the geometry of the gasket changes with pressure, there exists an unknown but systematic uncertainty of this order in magnetic-field determination. The data in Fig. 4(b) for $g_{\parallel}$ have been corrected by a constant value equal to the shift at zero pressure. The unknown geometrical change at the higher pressures adds an estimated uncertainty of 2×10^{-4} in $g_{\parallel}$ for all points at pressure. Since the random errors illustrated in Fig. 4(b) suggest essentially no change in $g_{\parallel}$ with pressure, we suggest that at most $g_{\parallel}$ experiences a fractional change of $\pm 2 \times 10^{-4}$ at 60 kilobars. Comparison with the previous nonhydrostatic data will be made later.

The line-width data presented in Fig. 4(c) demonstrate the most significant advantage of the hydrostatic feature of this system. The width reported is the peak-to-peak width of the differential signal from the absorption peak. In several attempts to use thicker samples the anvil came in touch with the sample as pressure was increased. The widths of lines one and three immediately increase by 50%–100%, indicating the high sensitivity of those lines to stress. If the load is increased further, these lines completely disappear, and the sample is crushed. The small variation of line width with pressure demonstrated by the data in Fig. 4(c) represents a measurable, physically meaningful, line-width variation that is related to the changing dynamical characteristics of the ruby. The scatter about the dashed lines shown is approximately 0.5% of the line width for the $(+3/2 \rightarrow +1/2)$ line, 1% for the $(-1/2 \rightarrow +1/2)$ line, but approximately 2% for the $(+1/2 \rightarrow +3/2)$ line. We have no explanation for this variation in precision, but we note that this variation is approximately the ratio of the magnetic fields of the lines and is also comparable to the orientational sensitivity of the lines.

As is well known, much greater care must be exercised when studying line profiles and line widths than when studying line positions. When cutting and polishing very thin samples from the same parent crystal of ruby, line widths of the $(+1/2 \rightarrow +3/2)$ and $(+3/2 \rightarrow +1/2)$ lines will vary by as much as 30% depending upon grinding and polishing procedures and size of sample. Line shapes are also drastically asymmetrical for the most broadened lines and not totally symmetric for any lines when samples are simply ground and polished. These variations are caused by inhomogeneous strain states in the sample resulting from the abrasion and are greater for smaller samples. The samples used here were all "annealed" by heating to a white heat near to but below the melting temperature after the crystal was shaped. This annealing is accomplished by placing the shaped ruby crystal inside an alumina tube and heating the tube with an acetylene torch until the surface of the tube is flame polished. Samples so annealed exhibited reproducible line widths, and these line widths are slightly narrower than the narrowest of any samples not annealed. Lines from the annealed samples were totally symmetric to within experimental detection and remained symmetric at all pressures. Without this care in annealing, the small changes observed due to hydrostatic pressure effects would be insignificant.

IV. LIMITATIONS AND DISCUSSION

When one considers the use of any apparatus in experimental studies, one needs to evaluate its strengths

and limitations relative to other available techniques. We have presented an ESR system capable of measurements in a hydrostatic environment to several times higher pressures than previous hydrostatic systems and with pressure-measurement sensitivity consistent with the best pressure measurements in this higher-pressure range. We have also provided some limited temperature capabilities. Thus, we have greatly extended the thermodynamic region over which meaningful ESR measurements can be made, and have demonstrated that very little degradation of the ESR data is inherent due to the pressure apparatus, except that due to limited sample size. We must, however, note the limitations of this system which are related to the pressure-generating and pressure-measuring systems.

When pressures above 25 kilobars are used, the sapphire cavity often develops cracks upon pressure release, and the cavity cannot be used again. Once applied, however, the higher pressures can be maintained indefinitely. Repeated measurements to pressures of 25–30 kilobars can be made without cracking the sapphire anvils. Development of small cracks in the sapphire apparently does not decrease the Q of the cavity, but if cracks develop into the sample region, loss of the liquid results, and the sample is crushed. One must recognize that there is a qualitative difference in pressure generation and measurement technique between the pressure attainable in a bomb-type system (15 kilobars limit) and the much higher pressure discussed herein. Of significance is the pressure control and measurement sensitivity. In a bomb-type apparatus unique pressures (such as a phase transition) can be approached and measured with a sensitivity of approximately one bar or less, whereas the control sensitivity in the present system is 50–100 times that large, and the measurement sensitivity is 200–300 times that value. Furthermore, in this anvil-type apparatus there is poor correlation between the applied load and the internal pressures when pressure cycling occurs or when temperature excursions are made. This situation makes continuous internal pressure measurement necessary. These conditions imply that the present system is very suitable for measurement of variations of spin-Hamiltonian parameters as well as measurement of line widths with pressure and temperature since the parameters are continuous and can be measured at any arbitrary number of points within the pressure range of interest. The system is not totally suitable for detailed study of critical behavior since specific pressures with fine pressure and temperature control must be attainable.

In the previous very high-pressure system developed in this laboratory the polycrystalline Al_2O_3-anvil cavity which was used contained impurities which caused some noise and extraneous resonances. The impurity level is much lower in the single-crystal cavity. The single-crystal sapphire cavity cylinders used in this system have been obtained from both Crystal Systems Company and from Linde Corporation. Crystals from both sources have consistent pressure capabilities, but the Crystal Systems sapphire yields only one observable impurity resonance at approximately 1500 G, whereas the Linde sapphire yields a more complex impurity spectrum.

The presence of the ruby fragment used for the pressure measurement as an impurity in the ESR sample chamber has not been a serious problem. The ruby fragment required for the fluorescence is very small and thus gives a very weak signal. Furthermore, ruby has a very simple ESR pattern. We originally had planned to orient the ruby used for pressure calibration in each sample in order to know precisely the position of each ruby ESR line, but we found this precaution not generally necessary.

One of the most serious limitations of the system is the small sample volume. Furthermore, the sample must be smaller at the higher pressures as indicated above. The ESR sensitivity of the system has been higher than expected, however. In practice we are able to make measurements on smaller samples than those usable in the Varian air cavity. This enhancement of sensitivity is probably associated with a cavity-filling factor. Since the volume of the cavity is reduced by approximately a factor of 10, the same size sample occupies a ten times larger fraction of the total cavity. The samples from which the data in Fig. 4 were taken were 0.6 mm in diameter by 0.1 mm thick and contained approximately 4×10^{14} spins. These samples yield very sizeable signals. Samples with 4×10^{13} total spins could be studied with appropriate care, and the sensitivity of the pressure cell appears to be very nearly equivalent to the maximum sensitivity of 2×10^{11} ΔH specified for the Varian system. In order to utilize the full sample chamber volume, it is wise to shape the sample to a thin disk of uniform thickness if possible.

In practice the experimental line intensities increase with applied load due to apparently improved electrical and geometrical configuration of the microwave cavity near the sample itself. The **E** and **B** fields of the cavity penetrate out through the hole provided in the silvered wall for placing the sample. This penetration depends upon the thickness of the gasket and the electrical conduction paths in the area. The Inconel gasket is a high-resistance metal, and as it gets thinner, the cavity wall currents, which are high in the region of the sample, are less perturbed than when a thicker gasket exists. We have observed almost a twofold signal increase due to this effect. The increase is not related to pressure in the sample directly since it remains on decreasing load when the gasket is still thin but the internal pressure has returned to zero. These small changes in cavity configuration and current are also the cause of much of the small mode frequency change observed with increasing load.

The ESR data presented for ruby illustrate most dramatically the improved precision and accuracy available at these higher pressures in this hydrostatic system. The error flags in Fig. 4 are less than 10% of the flags for the quasi-hydrostatic data. It is, however, significant that the nonhydrostatic stress does not

systematically change the energy difference. The line broadening experienced in the nonhydrostatic data is many times that observed in the hydrostatic environment and is indicative in the nonhydrostatic case only of the nonhomogeneity of the sample as measured by local field around the individual Cr^{3+} ions. The precision of the present data allows one to observe not only the pressure derivative $d\delta/dP$ but also the curvature $d^2\delta/dP^2$.

The value of $d\delta/dP = B = (6.70 + 0.08) \times 10^{-4}\,\mathrm{cm}^{-1}$ kilobar^{-1} differs significantly from both the earlier hydrostatic value[15,16] of $(7.2 + 0.1) \times 10^{-4}$ and the previous nonhydrostatic value of $(6.0 + 0.4) \times 10^{-4}$ reported from this laboratory. The error in the nonhydrostatic value is due only to the neglect of the quadratic term in the expansion since the data points essentially fall on the present hydrostatic curve. We offer no explanation for the discrepancy with the earlier hydrostatic data except to note that a much higher precision both in ESR and pressure data is required over the smaller pressure range to determine a precise slope and that our accuracy is consistent with the atmospheric operation of the ESR spectrometer. We note that the small correction for the susceptibility of the gasket discussed relative to the $g_{\|}$ data does not apply to the $\delta(P)$ data since δ depends on ratios of H_1/H_2 and H_3/H_2 rather than on an absolute value of H as $g_{\|}$ does.

The original nonhydrostatic data indicated a possible change in $g_{\|}$ with pressure but with an uncertainty approximately 20 times the uncertainty in these present measurements. We conclude that $g_{\|}$ exhibits a fractional change less than $\pm 2 \times 10^{-4}$ at 60 kilobars. Since our basic objective is not the study of the ruby itself, we will not discuss the significance of the line widths or the microscopic interpretations of the variation in δ or $g_{\|}$.

ACKNOWLEDGMENTS

We would like to thank Herbert Kirchoff who constructed the pressure cell, the Eulerian cradle, and the precision laser mount, Dr. Howard Vanfleet for considerable help and several stimulating conversations, and Mohamed El-Gamal for performing some of the measurements on ruby.

[a] A significant portion of this work was part of the doctoral dissertation of Som D. Tyagi, Brigham Young University (1976).
[b] Current Address: Department of Physics, Drexel University, Philadelphia, PA, 19104.

[1] W. M. Walsh, Jr. and W. Bloembergen, Phys. Rev. **107,** 904 (1957).
[2] J. Stankowski *et al.*, Rev. Sci. Instrum. **47,** 128 (1976).
[3] L. Rimai, T. Deutsch, and B. D. Silverman, Phys. Rev. **133,** A1123 (1964).
[4] J. H. Gardner *et al.*, Rev. Sci. Instrum. **34,** 1043 (1964).
[5] H. M. Nelson, D. B. Larson, and J. H. Gardner. J. Chem. Phys. **47,** 1994 (1967).
[6] J. D. Barnett, S. Block, and G. J. Piermarini, Rev. Sci. Instrum. **44,** 1 (1973).
[7] G. J. Piermarini, S. Block, J. D. Barnett, and R. A. Forman. J. Appl. Phys. **46,** 2774 (1975).
[8] C. Weir, S. Block, and G. Piermarini. J. Res. Natl. Bur. Stand. (U.S.) **69c**, 275 (1965).
[9] R. S. Hawke, K. Syassen, and W. B. Holzapfel, Rev. Sci. Instrum. **45,** 1598 (1974).
[10] P. F. Liao and S. R. Hartmann, Phys. Rev. B **8,** 69 (1973).
[11] M. M. Zaripov and Iu. Ia. Shamoniu, Sov. Phys. JETP **3,** 171 (1956).
[12] J. E. Geusic, Phys. Rev. **102,** 1252 (1956).
[13] Toshiaki Tatsukawa, Masasi Inque, and Hisao Yagi, J. Phys. Soc. Jpn. **36,** 908 (1974).
[14] W. J. C. Grant and M. W. P. Strandberg, Phys. Rev. **135,** A727 (1964).
[15] A. F. Clark, R. H. Sands, and C. K. Kikuchi, Tech. Rept. ORA Project 06029, 1964.
[16] T. I. Alaeva, L. F. Vereshchagin, and E. N. Yakoviev, Sov. Phys. Solid State **11,** 398 (1969).